Transition Metal Complexes with Sulfur Ligands. 136.[1] Enforced Trans Coordination of Thiolate Donors in Electron Rich Iron, Ruthenium, and Nickel [M(L)(py$N_2H_2S_2$)] and [M(L)(pyS_4)] Complexes (L = CO, PPh_3, DMSO) (py$N_2H_2S_2^{2-}$ = 2,6-Bis(2-mercaptophenylamino)dimethylpyridine(2−); pyS_4^{2-} = 2,6-Bis(2-mercaptophenylthio)dimethylpyridine(2−))

Dieter Sellmann,* Jürgen Utz, and Frank W. Heinemann

Institut für Anorganische Chemie der Universität Erlangen-Nürnberg, Egerlandstrasse 1, D-91058 Erlangen, Germany

Received February 10, 1999

In the course of a systematic study of transition metal complexes exhibiting three properties, electron rich metal centers, core structures with trans thiolate donors, and the capability to bind nitrogenase related small molecules, the pentadentate ligands py$N_2H_2S_2$-H_2 (=2,6-bis(2-mercaptophenylamino)dimethylpyridine) and pyS_4-H_2 (=2,6-bis(2-mercaptophenylthio)dimethylpyridine) have been synthesized. Alkylation of 2(3*H*)-benzothiazolone by 2,6-bis[(tosyloxy)methyl]pyridine and subsequent alkaline hydrolysis yielded py$N_2H_2S_2$-H_2 (**3**). Template alkylation of $[Ni(S_2C_6H_4)_2]^{2-}$ (**6**) by 2,6-bis[(tosyloxy)methyl]pyridine gave $[Ni(pyS_4)]_2$ (**7**) whose acidic hydrolysis yielded pyS_4-H_2·HCl (**9**). The reaction of Fe(II) salts with py$N_2H_2S_2^{2-}$ gave [Fe(py$N_2H_2S_2$)] (**10**). Five-coordinate **10** is paramagnetic (μ_{eff} (293 K) = 5.34 μ_B), has a trigonal bipyramidal structure, and coordinates CO to give diamagnetic [Fe(CO)(py$N_2H_2S_2$)] (**11**). Although the ν(CO) of **11** (1928 cm^{-1} (KBr)) indicates electron rich Fe centers and strong Fe−CO bonds, **11** readily dissociated CO in solution. Reactions of py$N_2H_2S_2^{2-}$ with ruthenium precursor complexes yielded diamagnetic [Ru(L)(py$N_2H_2S_2$)], (L = DMSO (**12**), PPh_3 (**13**), or CO (**14**)) which have practically substitution inert Ru−L bonds. Only **12** could be converted into **14** under drastic conditions (140 bar CO, 120 °C, 12 h, THF). Methylation of the thiolate donors to give [Ru(L)(py$N_2H_2S_2$-Me_2)]I_2 (L = DMSO (**15**) and PPh_3 (**16**)) did not labilize the Ru−L bonds. The reaction of Fe(II) salts with pyS_4^{2-} in the presence of CO yielded [Fe(CO)(pyS_4)] (**17**). Complex **17** has a higher ν(CO) (1955 cm^{-1} in KBr) than **11** but is stable toward Fe−CO dissociation. The spectroscopic data of all synthesized complexes and X-ray structure analyses of **7**, **10**, **13**, **15**, **16**, and **17** showed that all six-coordinate [M(L)(py$N_2H_2S_2$)] and [M(L)(pyS_4)] complexes uniformly have C_2 symmetrical core structures and trans thiolate donors, thus differing from analogous complexes of pentadentate $N_xH_xS_y^{2-}$ ligands ($x + y = 5$) whose $[MN_xS_y]$ cores exhibit either C_S or C_1 symmetry and cis or trans thiolate donors. The ν(CO) frequencies in homologous [Fe(CO)($N_xH_xS_y$)] complexes ($x + y = 5$) showed that exchange of aromatic thioether S for amine NH donors considerably increases the electron density at the iron centers. A minor influence was observed for the exchange of aliphatic thioether S for NH donors or changes of the $[FeN_xS_y]$ core structures.

Introduction

Metal oxidation state, type, and number of donor atoms and core structures are major factors which determine structure−function relationships of transition metal complexes.[2,3] Structure−function relationships can also be expected to control the ability of metal complex fragments to coordinate and activate or stabilize nitrogenase related small molecules such as N_2, N_2H_2, N_2H_4, NH_3, CO, H_2, etc.[4]

In our quest for transition metal complexes binding these molecules we have found that the [Fe(NHS_4)] fragment exists in the two diastereomeric forms **A** and **B** (Scheme 1). Diastereomer **A** yields high-spin [Fe(L)(NHS_4)] complexes with L = N_2H_4, NH_3, and MeOH, diastereomer **B** forms low-spin [Fe(L)(NHS_4)] complexes with L = CO, N_2H_2, and PR_3. Neither diastereomer **A** or **B**, however, binds N_2.[5−9]

Anticipating that a higher electron density at the Fe centers favors the binding of N_2,[10] we have tried to systematically exchange the potentially π-accepting S thioether functions[9] of the NHS_4^{2-} ligand for σ-donor NH amine functions. A series of pentadentate $N_xH_xS_y$-H_2 ligands ($x + y = 5$) was prepared (Scheme 1).[1,7,11] The characteristic and, for our goals, important

* To whom correspondence should be addressed.

(1) For part 135, see: Sellmann, D.; Utz, J.; Heinemann, F. W. *Eur. J. Inorg. Chem.* **1999**, 341.
(2) Mellor, D. P. In *Chelating Agents and Metal Chelates*; Dwyer, F. P., Mellor, D. P., Eds.; Academic Press: New York, 1964; p 44.
(3) Burger, K. In *Biocoordination Chemistry*; Burger, K., Ed.; Ellis Horwood: New York, 1990; p 11.
(4) Sellmann, D. *Angew. Chem.* **1993**, *105*, 67; *Angew. Chem., Int. Ed. Engl.* **1993**, *32*, 64.
(5) Sellmann, D.; Soglowek, W.; Knoch, F.; Ritter, G.; Dengler, J. *Inorg. Chem.* **1992**, *31*, 3711.
(6) Sellmann, D.; Soglowek, W.; Knoch, F.; Moll, M. *Angew. Chem.* **1989**, *101*, 1244; *Angew. Chem., Int. Ed. Engl.* **1989**, *28*, 1271.
(7) Sellmann, D.; Kunstmann, H.; Knoch, F.; Moll, M. *Inorg. Chem.* **1988**, *27*, 4183.
(8) Sellmann, D.; Hofmann, T.; Knoch, F. *Inorg. Chim. Acta* **1994**, *224*, 61.
(9) Sellmann, D.; Sutter, J. *Acc. Chem. Res.* **1997**, *30*, 460.
(10) Henderson, R. A.; Leigh, G. J.; Pickett, C. J. *Adv. Inorg. Chem. Radiochem.* **1983**, *27*, 245.

10.1021/ic990169h CCC: $18.00
Published on Web 10/21/1999

Scheme 1. Ligands and Core Structures of Metal Complex Fragments

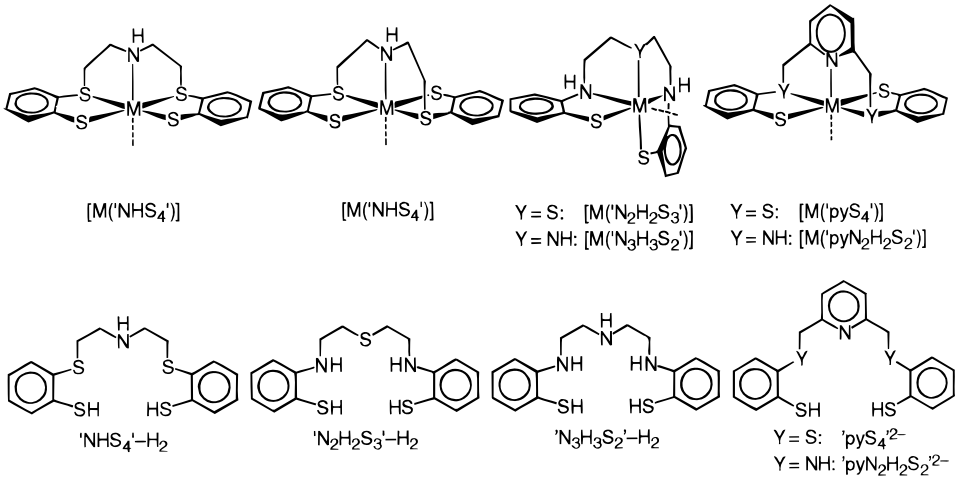

feature common to all these ligands are the terminal thiolate functions. The ν(CO) bands of the iron carbonyl complexes [Fe(CO)($N_2H_2S_3$)] and [Fe(CO)($N_3H_3S_2$)] ($\sim$1930 cm^{-1}) indeed indicate a higher electron density at the iron centers than in [Fe(CO)(NHS_4)] (1960 cm^{-1}). However, these CO complexes are labile in solution, readily dissociate CO, and exhibit the core structure **C**. This structure, due to its cis thiolate donors, is unfit to stabilize reactive species such as diazene via bifurcated N−H···(S)$_2$ bridges, which are a major stabilization factor of diazene in complexes such as [μ-N_2H_2{Fe(NHS_4)}$_2$] and related species.[6,9]

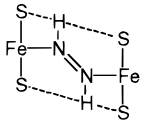

Finally, the aromatic NH functions of [M(L)($N_2H_2S_3$)] and [M(L)($N_3H_3S_2$)] complexes readily deprotonate to give amide donors, possibly accounting for the limited coordination chemistry of [Fe($N_2H_2S_3$)] and [Fe($N_3H_3S_2$)] complex fragments that bind only CO. Analogous [Ru(L)($N_2H_2S_3$)] and [Ru(L)($N_3H_3S_2$)] complexes, which could only be obtained with L = PR_3 and NO^+, also exhibit the core structure **C**, and proved virtually substitution inert. For these reasons we have now tried to exchange the conformationally flexible central NH(C_2H_4)$_2$ bridge in the $N_xH_xS_y$-H_2 ligands by the rigid 2,6-bismethylenepyridine entity (C_5H_3N)(CH_2)$_2$ ([py(CH_2)$_2$]).[12] The goal was to introduce steric constraints in the target ligands $pyN_2H_2S_2$-H_2 and pyS_4-H_2, to enforce meridional coordination of the three central donors and trans coordination of the terminal thiolate donors, such that the resulting core structure **D** compares to the diastereomer **B** of [Fe(NHS_4)].

When our studies were in progress, H. Vahrenkamp et al. published the synthesis of $pyN_2H_2S_2$-H_2 and one of its zinc complexes.[13] We found that [Fe(CO)($pyN_2H_2S_2$)] exhibits the anticipated core structure **D** and a ν(CO) frequency (1928 cm^{-1}) indicating a high electron density at the iron center. Nevertheless, [Fe(CO)($pyN_2H_2S_2$)] proved as labile as [Fe(CO)($N_2H_2S_3$)] and [Fe(CO)($N_3H_3S_2$)] with respect to CO dissociation. This was a major reason to synthesize the pyS_4-H_2 ligand and to investigate its coordination to Fe(II) centers in orienting experiments.

Experimental Section

General Methods. Unless noted otherwise, all procedures were carried out under N_2 at room temperature using Schlenk techniques. Solvents were dried and distilled before use. As far as possible the reactions were monitored by IR spectroscopy. Spectra were recorded on the following instruments: IR, Perkin-Elmer 16 PC FT-IR; NMR, JEOL JNM-GX 270 and JNM-EX 270; mass spectra, Varian MAT 212 and JEOL JMS 700. [$RuCl_2(PPh_3)_3$],[14] [$RuCl_2(DMSO)_4$],[15] [Ru(H)(Cl)(CO)(PCy_3)$_2$],[16] 1,2-benzenedithiol,[17] 2,6-bis[(tosyloxy)methyl]-pyridine,[18] and 2(3*H*)-benzothiazolone[19] were prepared by literature methods. Hydrazine was obtained by 2-fold distillation of N_2H_4·H_2O over solid potassium hydroxide under reduced pressure.

Syntheses. *Alkylation of 2(3H)-Benzothiazolone (**1**) by 2,6-Bis-[(tosyloxy)methyl]pyridine To Give **2**.* A suspension of 2(3*H*)-benzothiazolone (**1**) (0.34 g, 2.25 mmol) and K_2CO_3 (0.38 g, 2.75 mmol) in 2-butanone (20 mL) was refluxed for 30 min and then combined with a suspension of 2,6-bis[(tosyloxy)methyl]pyridine (0.51 g, 1.14 mmol) in 2-butanone (20 mL). The reaction mixture was refluxed for another 14 h and evaporated to dryness. The white residue was dissolved in boiling EtOH (20 mL). Addition of H_2O (40 mL) precipitated a white powder, which was separated, recrystallized from EtOH, and dried in vacuo yielding 0.33 g (72%) of **2**. IR (KBr, cm^{-1}): 1682 vs ν(CO). ^{1}H NMR (DMSO-d_6, ppm, 269.6 MHz): δ = 7.80−7.01 (m, 11 H, C*H*(aryl)), 5.17 (s, 4 H, CH_2). ^{13}C{^{1}H} NMR (DMSO-d_6, ppm, 67.7 MHz): δ = 169.0 (*C*O), 154.7, 138.4, 136.9, 126.4, 123.1, 122.8, 121.3, 120.9, 111.5 (*C*(aryl)), 46.9 (*C*H$_2$). MS (FD, DMSO): *m*/*z* 405 [**2**]$^+$. Anal. Calcd for $C_{21}H_{15}N_3O_2S_2$ (405.50): C, 62.20; H, 3.73; N, 10.36; S, 15.82. Found: C, 62.42; H, 3.91; N, 10.45; S, 15.73.

*$pyN_2H_2S_2$-H_2 (**3**).* A solution of NaOH (0.26 g, 6.50 mmol) in H_2O (20 mL) was added to a suspension of **2** (0.33 g, 0.81 mmol) in EtOH (20 mL). The mixture was refluxed for 14 h, cooled to room temperature, and concentrated hydrochloric acid was added until pH 5 was reached. The resulting solution was concentrated in volume to one-half, diluted with H_2O (20 mL), and extracted with CH_2Cl_2 (50 mL). The combined CH_2Cl_2 phases were dried with anhydrous Na_2SO_4, filtered, and evaporated to dryness yielding **3** (0.28 g, 97%) as a viscous yellow oil which solidified at room temperature. IR (KBr, cm^{-1}): 3414

(11) Sellmann, D.; Utz, J.; Heinemann, F. W. *Inorg. Chem.* **1999**, *38*, 459.
(12) Rothermel, G. L., Jr.; Miao, L.; Hill, A. L.; Jackels, S. C. *Inorg. Chem.* **1992**, *31*, 4854.
(13) Brand, U.; Burth, R.; Vahrenkamp, H. *Inorg. Chem.* **1996**, *35*, 1083.
(14) Stephenson, T. A.; Wilkinson, G. *J. Inorg. Nucl. Chem.* **1966**, *28*, 945.
(15) Evans, I. P.; Spencer, A.; Wilkinson, G. *J. Chem. Soc., Dalton Trans.* **1973**, 204.
(16) Sellmann, D.; Ruf, R.; Knoch, F.; Moll, M. *Inorg. Chem.* **1995**, *34*, 4745.
(17) Degani, J.; Fochi, R. *Synthesis* **1976**, *7*, 471.
(18) Bradshaw, J. S.; Huszthy, P.; McDaniel, C. W.; Zhu, J. Y.; Dalley, N. K.; Izatt, R. M. *J. Org. Chem.* **1990**, *55*, 3129.
(19) Hunter, R. F. *J. Chem. Soc.* **1930**, 125.

w, 3395, 3374 m ν(NH), 2524, 2505 w ν(SH). ^{1}H NMR (CD_2Cl_2, ppm, 269.6 MHz): δ = 7.51−6.65 (m, 11 H, C*H*(aryl)), 5.98−4.55 (s, br, 2 H, N*H*), 4.41 (s, 4 H, CH_2), 4.15−2.65 (s, br, 2 H, S*H*). ^{13}C{^{1}H} NMR (CD_2Cl_2, ppm, 67.7 MHz): δ = 157.9, 148.4, 137.5, 135.2, 129.6, 120.2, 117.4, 112.1, 111.0 (*C*(aryl)), 49.2 (*C*H$_3$). MS (FD, CH_2Cl_2): *m*/*z* 706 [(py$N_2H_2S_2$-H_2)$_2$]$^+$, 353 [py$N_2H_2S_2$-H_2]$^+$. Anal. Calcd for $C_{19}H_{19}N_3S_2$ (353.51): C, 64.55; H, 5.42; N, 11.89; S, 18.14. Found: C, 64.30; H, 5.54; N, 11.89; S, 19.71.

*py$N_2H_2S_2$-Me$_2$ (**4**)*. MeI (0.50 mL, 8.03 mmol) was added to a solution of py$N_2H_2S_2$-H_2 (**3**) (1.09 g, 3.08 mmol) and LiOMe (6.20 mmol, 6.20 mL of a 1 M solution in MeOH) in THF (20 mL). The reaction mixture was stirred for 16 h and then evaporated to dryness. The residue was redissolved in a 1:1 mixture (80 mL) of H_2O and CH_2Cl_2. The CH_2Cl_2 phase was separated, dried with anhydrous Na_2SO_4 and evaporated to dryness yielding **4** (1.00 g, 85%) as a yellow oil. ^{1}H NMR (CD_2Cl_2, ppm, 269.6 MHz): δ = 7.62 (t, 1 H, H$_\gamma$, pyridine), 7.42 (dd, 2 H, C$_6H_4$), 7.22 (d, 2 H, H$_\beta$, pyridine), 7.13 (dt, 2 H, C$_6H_4$), 6.67 (dt, 2 H, C$_6H_4$), 6.60 (d, 2 H, C$_6H_4$), 5.97 (t, 2 H, N*H*), 4.55 (d, 4 H, CH_2), 2.39 (s, 6 H, SCH_3). ^{13}C{^{1}H} NMR (CD_2Cl_2, ppm, 67.7 MHz): δ = 158.5, 148.2, 137.5, 133.9, 129.5, 120.6, 120.0, 117.4, 110.7 (*C*(aryl)), 49.5 (*C*H$_2$), 18.2 (S*C*H$_3$). MS (FD, THF): *m*/*z* 762 {[py$N_2H_2S_2$-Me$_2$]$_2$}$^+$, 381 [py$N_2H_2S_2$-Me$_2$]$^+$.

*py$N_2H_2S_2$-Me$_2$·2HCl (**5**)*. Concentrated hydrochloric acid (0.20 mL, 2.40 mmol) was added to a solution of py$N_2H_2S_2$-Me$_2$ (**4**) (0.42 g, 1.10 mmol) in MeOH (20 mL). After removal of the solvents the bright yellow residue was digested three times with CH_2Cl_2 (15 mL), and dried in vacuo to yield 0.47 g (90%) of **5**. ^{1}H NMR (DMSO-d_6, ppm, 269.6 MHz): δ = 9.75 (s, br, 4 H, N*H*), 8.35 (t, 1 H, H$_\gamma$, pyridine), 7.72 (d, 2 H, H$_\beta$, pyridine), 7.28 (d, 2 H, C$_6H_4$), 7.00 (t, 2 H, C$_6H_4$), 6.61 (t, 2 H, C$_6H_4$), 6.59 (d, 2 H, C$_6H_4$), 4.92 (s, 4 H, CH_2), 2.35 (s, 6 H, SCH_3). ^{13}C{^{1}H} NMR (DMSO-d_6, ppm, 67.7 MHz): δ = 155.6, 146.0, 146.0, 132.4, 128.6, 123.3, 120.6, 117.8, 110.3 (*C*(aryl)), 43.6 (*C*H$_2$), 17.2 (S*C*H$_3$). MS (FD, DMSO): *m*/*z* 381 [py$N_2H_2S_2$-Me$_2$]$^+$. Anal. Calcd for $C_{21}H_{25}Cl_2N_3S_2$·H_2O (472.51): C, 53.38; H, 5.76; N, 8.89; S, 13.57. Found: C, 53.54; H, 5.66; N, 8.71; S, 13.64.

*[Fe(py$N_2H_2S_2$)] (**10**)*. A solution of $FeCl_2$·$4H_2O$ (0.123 g, 0.617 mmol) in MeOH (15 mL) was added to a solution of py$N_2H_2S_2$-H_2 (**3**) (0.218 g, 0.617 mmol) and LiOMe (1.23 mmol, 1.23 mL of a 1 M solution in MeOH) in THF (20 mL) yielding a yellow suspension. After 30 min the yellow solid was separated, washed with THF and MeOH (20 mL each), and dried in vacuo yielding 0.247 g (98%) of **10**. IR (KBr, cm^{-1}): 3283 m, 3152 w, br ν(NH). MS (FD, DMSO): *m*/*z* 407 [Fe(py$N_2H_2S_2$)]$^+$. μ_{eff} (293 K) = 5.34 μ_B. Anal. Calcd for $C_{19}H_{17}FeN_3S_2$ (407.35): C, 56.02; H, 4.21; N, 10.32; S, 15.74. Found: C, 55.97; H, 4.21; N, 10.31; S, 16.23.

*[Fe(CO)(py$N_2H_2S_2$)] (**11**)*. CO was bubbled through a yellow suspension of [Fe(py$N_2H_2S_2$)] (**10**) (0.38 g, 0.49 mmol) in CH_2Cl_2 (30 mL) for 2 h. An orange solid resulted which was separated, washed with CH_2Cl_2 (20 mL), and dried in vacuo yielding 0.42 g (99%) of **11**. (**11** is obtained in equally high yields when the reaction mixture resulting in the synthesis of **10** is directly treated with CO for 2 h.) IR (KBr, cm^{-1}): 3280 w, 3176 w, br ν(NH), 1928 vs ν(CO). ^{1}H NMR (DMSO-d_6, ppm, 269.6 MHz): δ = 7.83 (t, 1 H, H$_\gamma$, pyridine), 7.54 (d, 2 H, H$_\beta$, pyridine), 7.03 (d, 2 H, C$_6H_4$), 6.97 (d, 2 H, C$_6H_4$), 6.70 (m, 4 H, C$_6H_4$), 6.50 (d, 2 H, N*H*), 4.54 (dd, 2 H, C*H*H), 4.22 (d, 2 H, CH*H*). ^{13}C{^{1}H} NMR (DMSO-d_6, ppm, 67.7 MHz): δ = 222.8 (*C*O), 158.1, 150.7, 149.2, 136.5, 129.4, 125.8, 124.6, 120.2, 119.7 (*C*(aryl)), 67.2 (*C*H$_2$). MS (FD, DMSO): *m*/*z* 407 [Fe(py$N_2H_2S_2$)]$^+$. Anal. Calcd for $C_{20}H_{17}FeN_3OS_2$·$0.25CH_2Cl_2$ (456.59): C, 53.27; H, 3.86; N, 9.20; S, 14.05. Found: C, 53.27; H, 4.09; N, 9.30; S, 14.24.

*[Ru(CO)(py$N_2H_2S_2$)] (**14**)*. (a) From [Ru(DMSO)(py$N_2H_2S_2$)] (**12**). In an autoclave, a yellow suspension of [Ru(DMSO)(py$N_2H_2S_2$)]·MeOH (**12**·MeOH) (0.100 g, 0.178 mmol) in THF (30 mL) was heated to 120 °C under 140 bar of CO pressure for 12 h. The yellow solid was separated, washed with THF and MeOH (30 mL each), and dried in vacuo yielding 0.078 g (88%) of **14**·0.5MeOH. (b) From [Ru(H)(Cl)(PCy$_3$)$_2$(CO)]. [Ru(H)(Cl)(PCy$_3$)$_2$(CO)] (0.206 g, 0.283 mmol) was added to a solution of py$N_2H_2S_2$-H_2 (**3**) (0.100 g, 0.283 mmol) and LiOMe (0.28 mmol, 0.28 mL of a 1 M solution in MeOH) in THF (25 mL). The reaction mixture was stirred for 3 h and the resulting red solution refluxed for 3 h. The precipitating yellow solid was separated, washed with THF and MeOH (10 mL each), and dried in vacuo yielding 0.02 g (14%) of **14**·0.5MeOH. IR (KBr, cm^{-1}): 3284, 3241 w ν(NH), 1927 vs ν(CO). ^{1}H NMR (DMSO-d_6, ppm, 269.6 MHz): δ = 8.37 (d, 2 H, N*H*), 7.73 (t, 1 H, H$_\gamma$, pyridine), 7.41 (d, 2 H, H$_\beta$, pyridine), 7.18−7.08 (m, 4 H, C$_6H_4$), 6.84−6.72 (m, 4 H, C$_6H_4$), 4.87 (dd, 2 H, C*H*H), 4.48 (d, 2 H, CH*H*). ^{13}C{^{1}H} NMR (DMSO-d_6, ppm, 67.7 MHz): δ = 207.2 (*C*O), 155.5, 149.9, 149.1, 137.3, 129.9, 126.1, 125.0, 120.5, 120.2 (*C*(aryl)), 69.2 (*C*H$_2$). MS (FD, DMSO, ^{102}Ru): *m*/*z* 481 [Ru(CO)(py$N_2H_2S_2$)]$^+$. Anal. Calcd for $C_{20}H_{17}N_3ORuS_2$·$0.5CH_3OH$ (496.60): C, 49.58; H, 3.86; N, 8.46. Found: C, 49.83; H, 4.14; N, 7.51.

*[Ru(PPh$_3$)(py$N_2H_2S_2$)] (**13**)*. [$RuCl_2$(PPh$_3$)$_3$] (0.814 g, 0.849 mmol) was added to a solution of py$N_2H_2S_2$-H_2 (**3**) (0.300 g, 0.849 mmol) and LiOMe (1.70 mmol, 1.70 mL of a 1 M solution in MeOH) in THF (20 mL). The reaction mixture was stirred for 15 h and then refluxed for 2 h yielding a red suspension. The red solid was separated, washed with MeOH and *n*-hexane (15 mL each), and dried in vacuo to yield 0.500 g (79%) of **13**·MeOH. IR (KBr, cm^{-1}): 3247, 3200 w ν(NH). ^{1}H NMR (DMSO-d_6, ppm, 269.6 MHz): δ = 7.47 (t, 1 H, H$_\gamma$, pyridine), 7.24 (d, 2 H, H$_\beta$, pyridine), 7.19−6.50 (m, 23 H, C$_6H_4$ and P(C$_6H_5$) superimposed), 6.25 (d, 2 H, N*H*), 4.81 (dd, 2 H, C*H*H), 4.31 (d, 2 H, CH*H*). ^{13}C{^{1}H} NMR (DMSO-d_6, ppm, 67.7 MHz): δ = 156.6, 151.5, 148.9 (*C*(aryl)), 137.5 (d, P(C$_6H_5$)), 133.8 (*C*(aryl)), 132.8 (d, P(C$_6H_5$)), 129.8 (*C*(aryl)), 127.7 (br, P(C$_6H_5$)), 126.9 (d, P(C$_6H_5$)), 125.2, 124.8, 119.3, 119.0 (*C*(aryl)), 69.9 (*C*H$_2$). ^{31}P{^{1}H} NMR (DMSO-d_6, ppm, 109.38 MHz): δ = 52.9 (s, *P*(C$_6H_5$)). MS (FD, DMSO, ^{102}Ru): *m*/*z* 715 [Ru(PPh$_3$)(py$N_2H_2S_2$)]$^+$. Anal. Calcd for $C_{37}H_{32}N_3PRuS_2$·CH_3OH (746.91): C, 61.11; H, 4.86; N, 5.63; S, 8.59. Found: C, 61.24; H, 4.65; N, 5.69; S, 8.70.

*[Ru(PPh$_3$)(py$N_2H_2S_2$-Me$_2$)]I_2 (**16**)*. (a) From [Ru(PPh$_3$)(py$N_2H_2S_2$)]·MeOH (**13**·MeOH). MeI (2.28 g, 16.1 mmol) was added to a red solution of [Ru(PPh$_3$)(py$N_2H_2S_2$)]·MeOH (**13**·MeOH) (0.21 g, 0.28 mmol) in THF (30 mL). The reaction mixture was stirred for 2 d yielding a beige suspension. The beige solid was separated, washed with THF and MeOH (10 mL each), recrystallized from CH_2Cl_2/*n*-hexane, and dried in vacuo to yield 0.23 g (80%) of **16**·$0.33CH_2Cl_2$. (b) From py$N_2H_2S_2$-Me$_2$ (**4**). py$N_2H_2S_2$-Me$_2$ (**4**) was synthesized in situ by addition of MeI (0.15 mL, 2.41 mmol) to a solution of py$N_2H_2S_2$-H_2 (**3**) (0.34 g, 0.96 mmol) and LiOMe (1.95 mmol, 1.95 mL of a 1 M solution in MeOH) in THF (20 mL) and stirring the reaction mixture for 12 h. After removal of the solvent the yellow residue was dissolved in THF (20 mL) and [$RuCl_2$(PPh$_3$)$_3$] (0.86 g, 0.90 mmol) was added. The brown reaction mixture was refluxed for 4 h yielding a green suspension, from which a beige solid could be separated. The beige solid was washed with THF and MeOH (10 mL each), recrystallized from CH_2Cl_2/*n*-hexane, and dried in vacuo to yield 0.65 g (70%) of **16**·$0.33CH_2Cl_2$. IR (KBr, cm^{-1}): 3190 w ν(NH). ^{1}H NMR (DMSO-d_6, ppm, 269.6 MHz): δ = 7.97 (t, 1 H, H$_\gamma$, pyridine), 7.93 (d, 2 H, N*H*), 7.58 (d, 2 H, H$_\beta$, pyridine), 7.47−7.03 (m, 23 H, C$_6H_4$ and P(C$_6H_5$)$_3$ superimposed), 5.56 (dd, 2 H, C*H*H), 4.58 (d, 2 H, CH*H*), 1.95 (s, 6 H, SCH_3). ^{13}C{^{1}H} NMR (DMSO-d_6, ppm, 67.7 MHz): δ = 158.9, 151.8, 138.3, 132.9 (d), 132.0, 131.5 (d), 131.0, 129.7, 128.8, 128.0 (d), 125.2, 121.4 (*C*(aryl)), 69.1 (*C*H$_2$), 22.0 (d, S*C*H$_3$). ^{31}P{^{1}H} NMR (DMSO-d_6, ppm, 109.38 MHz): δ = 39.2 (s, *P*(C$_6H_5$)). MS (FD, DMSO, ^{102}Ru): *m*/*z*] 745 [Ru(PPh$_3$)(py$N_2H_2S_2$-Me$_2$)]$^+$, 730 [Ru(PPh$_3$)(py$N_2H_2S_2$-Me)]$^+$, 715 [Ru(PPh$_3$)(py$N_2H_2S_2$)]$^+$. Anal. Calcd for $C_{39}H_{38}I_2N_3PRuS_2$·$0.33CH_2Cl_2$ (1027.05): C, 46.00; H, 3.79; N, 4.09; S, 6.24. Found: C, 45.89; H, 3.89; N, 4.14; S, 6.02.

*[Ru(DMSO)(py$N_2H_2S_2$)] (**12**)*. [$RuCl_2$(DMSO)$_4$] (0.137 g, 0.283 mmol) was added to a solution of py$N_2H_2S_2$-H_2 (**3**) (0.100 g, 0.283 mmol) and LiOMe (0.57 mmol, 0.57 mL of a 1 M solution in MeOH) in THF (25 mL). The reaction mixture was stirred for 15 h and then refluxed for 2 h. A yellow suspension resulted, from which the yellow solid was separated, washed with THF (20 mL), and dried in vacuo yielding 0.11 g (69%) of **12**·MeOH. IR (KBr, cm^{-1}): 3106 w, br ν(NH), 1011 s ν(SO). ^{1}H NMR (DMSO-d_6, ppm, 269.6 MHz): δ = 7.51 (t, 1 H, H$_\gamma$, pyridine), 7.47 (d, 2 H, N*H*), 7.24 (d, 2 H, H$_\beta$, pyridine), 7.22−7.14 (m, 4 H, C$_6H_4$), 6.77−6.64 (m, 4 H, C$_6H_4$), 4.68 (dd, 2 H, C*H*H), 4.28 (d, 2 H, CH*H*), 3.15 (s, 3 H, CH_3S(O)CH$_3$), 2.75 (s, 3 H, CH$_3$S(O)CH_3). ^{13}C{^{1}H} NMR (DMSO-d_6, ppm, 67.7 MHz): δ = 156.8, 150.6, 150.0, 134.2, 130.0, 125.6, 125.2, 119.7, 119.4 (*C*(aryl)), 68.7

(CH_2), 46.4, 44.2 (CH_3). MS (FD, DMSO, ^{102}Ru): *m/z* 906 [Ru(pyN$_2$H$_2$S$_2$)]$_2^+$, 453 [Ru(pyN$_2$H$_2$S$_2$)]$^+$. Anal. Calcd for $C_{21}H_{23}N_3ORuS_3 \cdot CH_3OH$ (562.75): C, 46.96; H, 4.84; N, 7.47. Found: C, 47.05; H, 5.01; N, 6.81.

*[Ru(DMSO)(pyN$_2$H$_2$S$_2$-Me$_2$)]I$_2$ (**15**).* MeI (0.1 mL, 1.6 mmol) was added to a yellow suspension of [Ru(DMSO)(pyN$_2$H$_2$S$_2$)]·MeOH (**12**·MeOH) (0.10 g, 0.178 mmol) in THF (30 mL). The reaction mixture was stirred for 2 d yielding a red suspension. The red solid was separated, washed with THF and MeOH (10 mL each), and dried in vacuo to yield 0.14 g (91%) of **15**·0.75THF. IR (KBr, cm^{-1}): 3260 w, br ν(NH), 1020 s ν(SO). ^{1}H NMR (DMSO-d_6, ppm, 269.6 MHz): δ = 10.18 (d, 2 H, N*H*), 8.00−7.41 (m, 11 H, C*H*(aryl)), 5.34 (dd, 2 H, C*H*H), 4.57 (d, 2 H, CH*H*), 3.00 (s, 3 H, CH_3S(O)CH$_3$), 2.74 (s, 3 H, CH$_3$S(O)CH_3), 2.08 (s, br, 6 H, CH_3). ^{13}C{^{1}H} NMR (DMSO-d_6, ppm, 67.7 MHz): δ = 157.9, 151.6, 138.6, 132.3, 131.9, 131.5, 129.4, 125.9, 121.9 (*C*(aryl)), 67.3 (CH_2), 46.6, 45.7 (CH_3, DMSO), 21.9 (CH_3). MS (FD, DMSO, ^{102}Ru): *m/z* 561 [Ru(DMSO)(pyN$_2$H$_2$S$_2$-Me$_2$)]$^+$. Anal. Calcd for $C_{23}H_{29}I_2N_3S_3RuO \cdot 0.75C_4H_8O$ (868.67): C, 35.95; H, 4.06; N, 4.84. Found: C, 35.83; H, 4.32; N, 4.91.

*[Ni(pyS$_4$)]$_2$ (**7**).* A solution of Ni(ac)$_2$·4H$_2$O (0.96 g, 3.84 mmol) in MeOH (15 mL) was added to a solution of 1,2-benzenedithiol (1.09 g, 7.68 mmol) and LiOMe (15.3 mmol, 15.3 mL of a 1 M solution in MeOH) in MeOH (20 mL). The resulting solution was combined with a suspension of 2,6-bis[(tosyloxy)methyl]pyridine (1.72 g, 3.84 mmol) in THF (30 mL) and stirred for 14 h. A brown-yellow suspension formed from which the brown solid was separated, washed with THF and MeOH (20 mL each), and dried in vacuo to yield 1.4 g (79%) of **7**·MeOH. IR (KBr, cm^{-1}): 3049 m ν(CH(aryl)), 1594 m, 1577 s ν(CC(aryl)), 738 s δ(CH(aryl)). MS (FD, DMSO, ^{58}Ni): *m/z* 443 [Ni(pyS$_4$)]$^+$. μ_{eff} (293 K) = 3.28 μ_B. Anal. Calcd for $C_{38}H_{30}N_2Ni_2S_8 \cdot CH_3OH$ (920.63): C, 50.88; H, 3.72; N, 3.04; S, 27.86. Found: C, 50.67; H, 3.44; N, 3.18; S, 26.13.

*pyS$_4$-H$_2$·HCl (**9**).* Concentrated hydrochloric acid (15 mL) was added to a suspension of [Ni(pyS$_4$)]$_2$·MeOH (**7**·MeOH) (1.0 g, 1.09 mmol) in CH_2Cl_2 (30 mL) and stirred for 1 h. The CH_2Cl_2 phase was separated from the green H_2O phase, dried with anhydrous Na_2SO_4, and evaporated to dryness yielding **9** (0.90 g, 98%) as a white foam. IR (KBr, cm^{-1}): 2550 m, br ν(NH) + ν(SH). ^{1}H NMR (CD_2Cl_2, ppm, 269.6 MHz): δ = 17.5 (s, br, 1 H, N*H*), 7.82 (t, 1 H, H$_\gamma$, pyridine), 7.35 (d, 2 H, C$_6H_4$), 7.32 (d, 2 H, C$_6H_4$), 7.21 (dt, 2 H, C$_6H_4$), 7.10 (d, 2 H, H$_\beta$, pyridine), 7.09 (dt, 2 H, C$_6H_4$), 4.59 (s, 4 H, CH_2), 4.34 (s, 2 H, S*H*). ^{13}C{^{1}H} NMR (CD_2Cl_2, ppm, 67.7 MHz): δ = 154.1, 143.8, 138.6, 135.4, 129.8, 129.6, 126.5, 125.0 (*C*(aryl)), 35.6 (CH_2). MS (FD, CH_2Cl_2): *m/z* 388 [pyS$_4$-H$_3$]$^+$. Anal. Calcd for $C_{19}H_{18}ClNS_4$ (424.08): C, 53.81; H, 4.28; N, 3.30; S, 30.25. Found: C, 53.70; H, 4.18; N, 3.32; S, 30.06.

*[Fe(CO)(pyS$_4$)] (**17**).* (a) From pyS$_4$-H$_2$·HCl (**9**). To a solution of pyS$_4$-H$_2$·HCl (**9**) (1.55 g, 3.65 mmol) and LiOMe (10.95 mmol, 10.95 mL of a 1 M solution in MeOH) in MeOH (20 mL), into which CO was continuously introduced, a solution of FeCl$_2$·4H$_2$O (0.726 g, 0.65 mmol) in MeOH (20 mL) was added. A red suspension resulted which was saturated with CO for another 2 h. The red solid was separated, washed with MeOH (30 mL), and dried in vacuo yielding 1.56 g (85%) of **17**·MeOH. (b) From 1,2-benzenedithiol. FeCl$_2$·4H$_2$O (0.87 g, 4.38 mmol) was added to a solution of 1,2-benzenedithiol (1.25 g, 8.79 mmol) and LiOMe (17.6 mmol, 17.6 mL of a 1 M solution in MeOH) in MeOH (40 mL). The resultant solution was saturated with CO for 3 h, combined with a solution of 2,6-bis[(tosyloxy)methyl]pyridine (1.97 g, 4.40 mmol) in THF (40 mL) and stirred for 24 h. After filtration the solution was concentrated in volume to one-half and diluted with MeOH (40 mL). A red solid precipitated which was separated, washed with MeOH (25 mL), and dried in vacuo to yield 1.20 g (55%) of **17**·MeOH. IR (KBr, cm^{-1}): 1955 vs ν(CO). ^{1}H NMR (THF-d_8, ppm, 269.6 MHz): δ = 7.63−7.56 (m, 2 H, C$_6H_4$), 7.44 (t, 1 H, H$_\gamma$, pyridine), 7.36−7.30 (m, 2 H, C$_6H_4$), 7.28 (d, 2 H, H$_\beta$, pyridine), 6.90−6.80 (m, 4 H, C$_6H_4$), 4.99 (d, 2 H, C*H*H), 4.68 (d, 2 H, CH*H*). ^{13}C{^{1}H} NMR (THF-d_8, ppm, 67.7 MHz): δ = 217.9 (*C*O), 159.2, 158.8, 136.5, 133.8, 132.3, 131.0, 128.8, 122.4, 122.0 (*C*(aryl)), 56.5 (CH_2). MS (FD, THF, [*m/z*]): 882 {[Fe(pyS$_4$)]$_2$}$^+$, 441 [Fe(pyS$_4$)]$^+$. Anal. Calcd for $C_{20}H_{15}FeNOS_4 \cdot CH_3OH$ (501.50): C, 50.30; H, 3.82; N, 2.79; S, 25.58. Found: C, 50.58; H, 3.60; N, 2.79; S, 25.76.

X-ray Structure Analysis of [Fe(pyN$_2$H$_2$S$_2$)] (10), [Ru(PPh$_3$)(pyN$_2$H$_2$S$_2$)]·1.5THF (13·1.5THF), [Ru(PPh$_3$)(pyN$_2$H$_2$S$_2$-Me$_2$)]I$_2$·CH$_2$Cl$_2$ (16·CH$_2$Cl$_2$), [Ru(DMSO)(pyN$_2$H$_2$S$_2$-Me$_2$)]I$_{0.5}$Cl$_{1.5}$·1.5CH$_2$Cl$_2$·0.5DMSO (15′·1.5CH$_2$Cl$_2$·0.5DMSO), [Fe(CO)(pyS$_4$)]·MeOH (17·MeOH), and [Ni(pyS$_4$)]$_2$ (7). Brown plates of [Fe(pyN$_2$H$_2$S$_2$)] (**10**) were obtained by layering a solution of pyN$_2$H$_2$S$_2$-H$_2$ (**3**) (0.109 g, 0.309 mmol) and LiOMe (0.62 mmol, 0.62 mL of a 1 M solution in MeOH) with a solution of FeCl$_2$·4H$_2$O (0.062 g, 0.309 mmol) in MeOH (20 mL). Green plates of [Ru(PPh$_3$)(pyN$_2$H$_2$S$_2$)]·1.5THF (**13**·1.5THF) formed when a saturated solution of **13** in THF was layered with Et$_2$O. Yellow-green blocks of [Ru(PPh$_3$)(pyN$_2$H$_2$S$_2$-Me$_2$)]I$_2$·CH$_2$Cl$_2$ (**16**·CH$_2$Cl$_2$) and green blocks of [Ru(DMSO)(pyN$_2$H$_2$S$_2$-Me$_2$)]I$_{0.5}$Cl$_{1.5}$·1.5CH$_2$Cl$_2$·0.5DMSO (**15′**·1.5CH$_2$Cl$_2$·0.5DMSO), respectively, were grown from a saturated solution of **16** in CH_2Cl_2 and **15** in a 10:1 mixture of CH_2Cl_2:DMSO which was layered with *n*-hexane. The Cl$^-$ ions located in the structure of **15′** are assumed to derive from the solvent CH_2Cl_2. The distribution of the counterions Cl$^-$ and I$^-$ was estimated from the X-ray data as well as from the elemental analysis (Anal. Calcd for [Ru(DMSO)(pyN$_2$H$_2$S$_2$-Me$_2$)]I$_{0.5}$Cl$_{1.5}$·1.5CH$_2$Cl$_2$·0.5DMSO: C, 36.30; H, 4.18; N, 4.98; S, 13.30. Found: C, 35.38; H, 4.22; N, 4.72; S, 12.95). Layering a saturated solution of **17** in THF with MeOH gave red columns of [Fe(CO)(pyS$_4$)]·MeOH (**17**·MeOH). Dark green plates of [Ni(pyS$_4$)]$_2$ (**7**) formed by layering a solution of pyS$_4$-H$_2$·HCl (**9**) (0.100 g, 0.236 mmol) and LiOMe (0.707 mmol, 0.707 mL of a 1 M solution in MeOH) in THF (30 mL) with a solution of Ni(ac)$_2$·4H$_2$O (0.059 g, 0.236 mmol) in MeOH (30 mL). Suitable single crystals were sealed under N_2 in glass capillaries and data were collected with a Siemens P4 diffractometer using Mo Kα radiation (λ = 71.073 pm, graphite monochromator). The structures were solved by direct methods (SHELXTL 5.03).[20] Full-matrix least-squares refinements were carried out on F^2-values (SHELXTL 5.03).[20] In the case of **10**, **16**, **15′**, and **7** all hydrogen atoms were calculated for ideal geometries. Their isotropic displacement parameters were tied to those of the adjacent carbon atoms by a factor of 1.5. **16** crystallizes with 1 molecule of CH_2Cl_2 per formula unit. **15′** crystallizes with 1.5 molecules of CH_2Cl_2 and 0.5 molecule of DMSO per formula unit. One CH_2Cl_2 as well as the DMSO molecule are located on a crystallographic mirror plane. The methyl group bound to S1 is disordered (C1A and C1B). Two sites could be refined, of which site A is occupied to 67(2)% and site B to 33(2)%. Compound **13** crystallizes with 1.5 molecules of THF per unit of which half a THF is disordered and located on an inversion center. The H atoms of the other THF molecule were calculated for ideal geometries. Their isotropic displacement parameters were tied to those of the adjacent carbon atoms by a factor of 1.5. For the disordered THF no H atoms were considered. All other H atoms of **13** as well as the H atoms of **17** were located in a difference Fourier synthesis and isotropically refined, except H2 (hydroxyl H atom) of **17**. For H2 of compound **17** both the coordinates and an isotropic displacement parameter were kept fixed during refinement. Table 1 contains selected crystallographic data of [Fe(pyN$_2$H$_2$S$_2$)] (**10**), [Ru(PPh$_3$)(pyN$_2$H$_2$S$_2$)]·1.5THF (**13**·1.5THF), [Ru(PPh$_3$)(pyN$_2$H$_2$S$_2$-Me$_2$)]I$_2$·CH$_2$Cl$_2$ (**16**·CH$_2$Cl$_2$), [Ru(DMSO)(pyN$_2$H$_2$S$_2$-Me$_2$)]I$_{0.5}$Cl$_{1.5}$·1.5CH$_2$Cl$_2$·0.5DMSO (**15′**·1.5CH$_2$Cl$_2$·0.5DMSO), [Fe(CO)(pyS$_4$)]·MeOH (**17**·MeOH), and [Ni(pyS$_4$)]$_2$ (**7**).

Results and Discussion

Syntheses of Ligands. The target ligands pyN$_2$H$_2$S$_2$-H$_2$ (**3**) and pyS$_4$-H$_2$ (**8**) were synthesized according to the routes indicated in Scheme 2.

For the synthesis of pyN$_2$H$_2$S$_2$-H$_2$ (**3**), we used the route which had proved successful in the preparation of the analogous N$_2$H$_2$S$_3$-H$_2$ and N$_3$H$_3$S$_2$-H$_2$ ligands.[1,11] Treatment of deprotonated 2(3*H*)-benzothiazolone (**1**) with 2,6-bis[(tosyloxy)methyl]-pyridine yielded **2**. Traces of byproducts resulting from *O*-alkylation of **1**[21] were removed by extracting the crude product with EtOH. The *N*-alkylation of **1** could be confirmed, in particular, by the CO group ^{13}C{^{1}H} NMR signal (δ = 169.0 ppm) and

(20) SHELXTL 5.03, Siemens Analytical X-ray Instruments, 1995.
(21) Cf.: Klein, G.; Prijs, B. *Helv. Chim. Acta* **1954**, *37*, 2057.

Table 1. Selected Crystallographic Data for [Fe($pyN_2H_2S_2$)] (**10**), [Ru(PPh_3)($pyN_2H_2S_2$)]·1.5THF (**13**·1.5THF), [Ru(PPh_3)($pyN_2H_2S_2$-Me_2)]I_2·CH_2Cl_2 (**16**·CH_2Cl_2), [Ru(DMSO)($pyN_2H_2S_2$-Me_2)]$I_{0.5}Cl_{1.5}$·1.5CH_2Cl_2·0.5DMSO (**15′**·1.5CH_2Cl_2·0.5DMSO), [Fe(CO)(pyS_4)]·MeOH (**17**·MeOH), and [Ni(pyS_4)]$_2$ (**7**)

compd	**10**	**13**·1.5THF	**16**·CH_2Cl_2	**15′**·1.5CH_2Cl_2·0.5DMSO	**17**·MeOH	**7**
formula	$C_{19}H_{17}FeN_3S_2$	$C_{43}H_{44}N_3O_{1.5}PRuS_2$	$C_{40}H_{40}Cl_2I_2N_3PRuS_2$	$C_{25.5}H_{35}Cl_{4.5}I_{0.5}N_3O_{1.5}RuS_{3.5}$	$C_{21}H_{19}FeNO_2S_4$	$C_{38}H_{30}N_2Ni_2S_8$
fw	407.33	820.96	1083.61	843.82	501.46	888.54
cryst size, mm^3	0.6 × 0.3 × 0.15	0.5 × 0.3 × 0.1	0.5 × 0.4 × 0.3	0.6 × 0.5 × 0.4	0.5 × 0.4 × 0.1	0.25 × 0.25 × 0.08
cryst system	monoclinic	triclinic	monoclinic	orthorhombic	triclinic	triclinic
space group	$P2_1/c$	$P\bar{1}$	$P2_1/n$	$Pnma$	$P\bar{1}$	$P\bar{1}$
a, pm	1290.3(3)	1086.1(2)	1059.5(1)	1852.9(6)	840.5(3)	837.6(2)
b, pm	960.3(5)	1355.2(3)	2342.6(2)	3337.2(6)	1126.0(6)	1064.9(2)
c, pm	1421.9(3)	1443.8(3)	1684.6(2)	1085.1(3)	1226.5(5)	1094.2(2)
α, deg	90	111.13(1)	90	90	67.97(4)	77.56(1)
β, deg	96.52(2)	103.74(1)	92.85(1)	90	84.30(3)	79.19(2)
γ, deg	90	97.82(1)	90	90	88.50(4)	81.24(2)
V, nm^3	1.750(1)	1.8670(7)	4.1760(7)	6.710(3)	1.0706(8)	0.9298(3)
Z	4	2	4	8	2	1
d_{calc}, g/cm^3	1.546	1.460	1.724	1.671	1.556	1.587
μ(Mo Kα), mm^{-1}	1.106	0.615	2.153	1.531	1.113	1.494
T, K	200	200	293	200	293	293
2θ range, deg	5.1 ≤ 2θ ≤ 55.2	4.2 ≤ 2θ ≤ 54.0	3.4 ≤ 2θ ≤ 54.5	4.3 ≤ 2θ ≤ 50.0	4.2 ≤ 2θ ≤ 54.3	4.9 ≤ 2θ ≤ 52.0
meas reflns	5720	9288	11229	7385	5365	4422
indep reflns	4051	7803	9207	6013	4737	3641
obsd reflns	2699	5250	5360	4458	3595	1162
refined params	226	598	462	384	334	226
R_1 (wR_2),[a,b] %	4.48 (12.66)	5.60 (12.81)	4.45 (11.99)	6.70 (19.02)	2.68 (6.86)	5.86 (14.86)
q[b]	0.0684	0.0328	0.0601	0.1000	0.0419	0.0457
r [b]		2.9082				

[a] $R_1 = [\sum||F_o| - |F_c||/\sum|F_o|]$ for $F > 4\sigma(F)$. [b] $wR_2 = [\sum[w(F_o^2 - F_c^2)^2]/\sum[w(F_o^2)^2]]^{1/2}$, where $w = 1/[\sigma^2(F_o^2) + (qP)^2 + rP]$ and $P = (F_o^2 + 2F_c^2)/3$.

the ν(CO) IR band at 1682 cm^{-1} (in KBr). Alkaline hydrolysis of **2** and subsequent acidification gave **3** in quantitative yield as a yellow oil, which solidified at room temperature. This preparation of **3** differs from that reported by Vahrenkamp et al., who used 2,6-pyridinedialdehyde and 1,2-aminothiophenol as starting materials.[13] The alkylation of **3** with MeI yielded the *S*-alkylated ligand $pyN_2H_2S_2$-Me_2 (**4**) as a yellow oil which was purified via its white dihydrochloride $pyN_2H_2S_2$-Me_2·2HCl (**5**).

For the synthesis of pyS_4-H_2 (**8**) nickel coordinated 1,2-benzenedithiolate $[Ni(S_2C_6H_4)_2]^{2-}$ (**6**)[22−26] was template alkylated with 2,6-bis[(tosyloxy)methyl]pyridine to give the dinuclear brown [Ni(pyS_4)]$_2$ (**7**). Complex **7** readily hydrolyzed when treated with hydrochloric acid to yield pyS_4-H_2 (**8**) which was isolated as the pyridinium salt pyS_4-H_2·HCl (**9**).

The compounds **2**, **3**, **4**, and **9** are well soluble in CH_2Cl_2 and THF, the salts **5** and **9** dissolve in MeOH while complex **7** is only sparingly soluble in hot DMF and DMSO. The compounds were characterized by elemental analysis and spectroscopic methods, and the molecular structure of **7** was determined by X-ray diffraction.

Syntheses and Reactions of Complexes. Scheme 3 summarizes the syntheses and reactions of $pyN_2H_2S_2^{2-}$ and pyS_4^{2-} complexes.

The reaction between Fe(II) salts and the $pyN_2H_2S_2^{2-}$ anion resulting from deprotonation of **3** with LiOMe gave yellow paramagnetic [Fe($pyN_2H_2S_2$)] (**10**) (μ_{eff} (293 K) = 5.34 μ_B). X-ray structure determination proved that **10** is mononuclear and exhibits a structure which had been aimed at by introducing the [py(CH_2)$_2$] bridge into the [FeN_3S_2] core. Complex **10** readily coordinated CO to give the C_2 symmetric and diamagnetic [Fe(CO)($pyN_2H_2S_2$)] (**11**) showing trans thiolate donors. The ν(CO) of **11** (1928 cm^{-1}) further indicated a high electron density at the Fe center and strong Fe−CO π-back-bonding. Although **11** is stable in solid state, it slowly dissociated CO in THF solution to give back **10**. CO dissociation had also been observed for the analogous [Fe(CO)($N_3H_3S_2$)]. In a further analogy to the [Fe($N_3H_3S_2$)] fragment, the [Fe($pyN_2H_2S_2$)] fragment did not add any other ligand than CO when treated, for example, with N_2H_4, NEt_4N_3, PMe_3, or N_2 under pressure.

These findings prompted us to proceed as in the previous investigations with the $N_2H_2S_3^{2-}$ and $N_3H_3S_2^{2-}$ ligands[1,11] and to also study those ruthenium complexes that could be expected to be less labile. Treatment of [$RuCl_2$(DMSO)$_4$] and [$RuCl_2$(PPh_3)$_3$] with $pyN_2H_2S_2^{2-}$ gave yellow [Ru(DMSO)($pyN_2H_2S_2$)] (**12**) and red [Ru(PPh_3)($pyN_2H_2S_2$)] (**13**), which proved not only less labile but virtually substitution inert. They did not exchange their DMSO or PPh_3 coligand for CO (50 bar, 20 °C, 2 d), N_2H_4 (N_2H_4 used as solvent, 40 °C, 1 d) or other nitrogen compounds at ambient or moderately elevated temperatures. Only under drastic conditions (140 bar of CO, 120 °C, 12 h) could DMSO/CO exchange be observed for **12** to give yellow [Ru(CO)($pyN_2H_2S_2$)] (**14**). As for the homologous [Fe(CO)($pyN_2H_2S_2$)] (**11**), the ν(CO) of **14** (1927 cm^{-1}) indicates a high electron density at the metal center and a strong M−CO bond, but in contrast to the Fe complex **11**, the ruthenium complex **14** is stable in solid state as well as in solution at ambient and elevated temperatures up to 100 °C. Complex **14** was also obtained from [Ru(H)(Cl)(CO)(PCy_3)$_2$] and $pyN_2H_2S_2^{2-}$, but only in very low yields. In an attempt to diminish the substitution inertness of [Ru(DMSO)($pyN_2H_2S_2$)] (**12**) and [Ru(PPh_3)($pyN_2H_2S_2$)] (**13**), the thiolate donors of **12** and **13** were alkylated with MeI,[27−30]

(22) Baker-Hawkes, M. J.; Billig, E.; Gray, H. B. *J. Am. Chem. Soc.* **1966**, *88*, 4870.
(23) Sellmann, D.; Fünfgelder, S.; Pöhlmann, G.; Knoch, F.; Moll, M. *Inorg. Chem.* **1990**, *29*, 4772.
(24) Sellmann, D.; Fünfgelder, S.; Knoch, F.; Moll, M. *Z. Naturforsch.* **1991**, *46b*, 1601.
(25) Sellmann, D.; Bail, P.; Knoch, F.; Moll, M. *Chem. Ber.* **1995**, *128*, 653.
(26) Sellmann, D.; Bail, P.; Knoch, F.; Moll, M. *Inorg. Chim. Acta* **1995**, *237*, 137.
(27) Sellmann, D.; Mahr, G.; Knoch, F.; Moll, M. *Inorg. Chim. Acta* **1994**, *224*, 45.

Scheme 2. Synthesis of Ligands

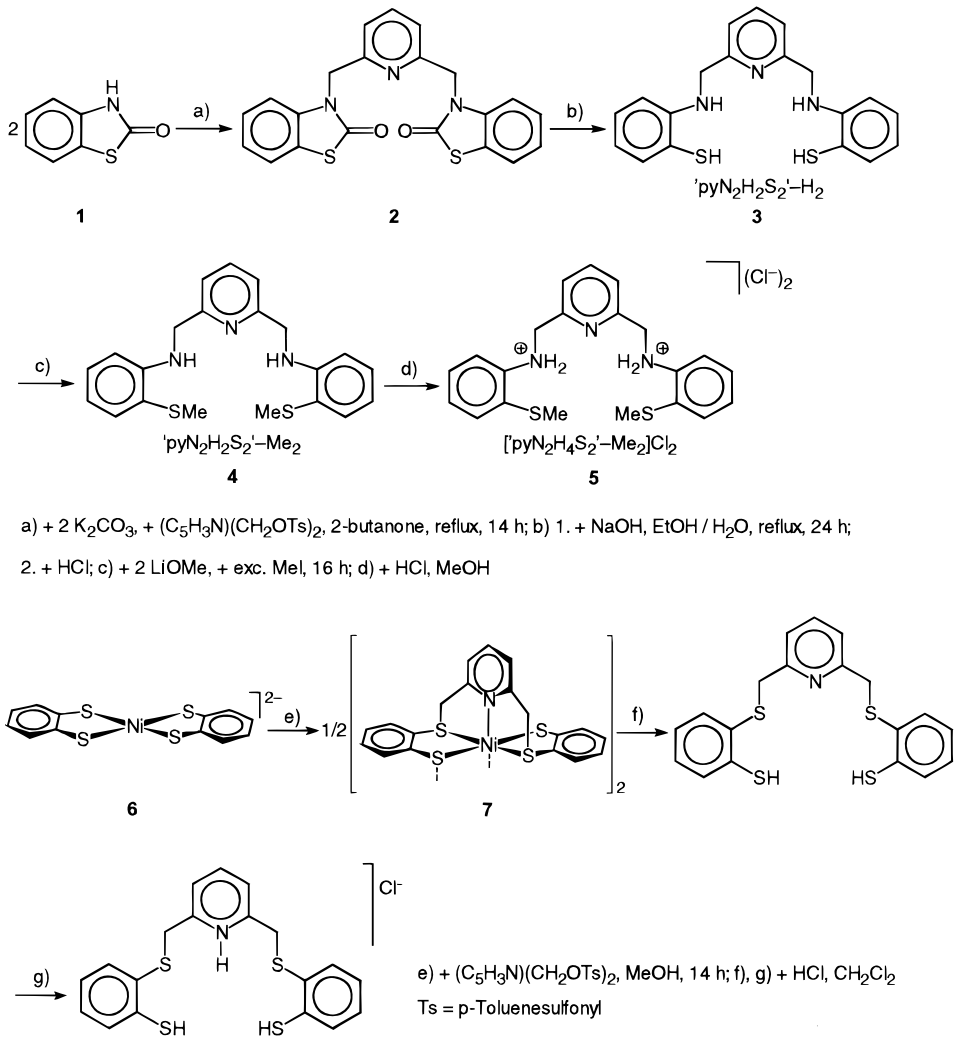

yielding the thioether derivatives [Ru(DMSO)($pyN_2H_2S_2$-Me_2)]I_2 (**15**) and [Ru(PPh_3)($pyN_2H_2S_2$-Me_2)]I_2 (**16**). Complexes **15** and **16** were fully characterized, but they proved as substitution inert as the precursor complexes **12** and **13**. For example, the PPh_3 ligand of [Ru(PPh_3)($pyN_2H_2S_2$-Me_2)]I_2 (**16**) could not be substituted by CO or N_2H_4. In these experiments it was noted that **16** is not deprotonated by N_2H_4 to give, e.g., [Ru(PPh_3)(pyN_2HS_2-Me_2)]I, thus differing from the related [Ru(PPh_3)($N_3H_3S_2$-Me_2)]I_2 which readily and reversibly deprotonates to give [Ru(PPh_3)($N_3H_2S_2$-Me_2)]I. This indicates a potentially important reactivity difference of [M(L)($N_3H_3S_2$)] and [M(L)($pyN_2H_2S_2$)] complexes. In fact, the core structure of [M(L)($pyN_2H_2S_2$)] complexes is expected to disfavor the deprotonation of the aromatic NH functions into amide functions, as the deprotonation requires a conversion of tetrahedral four-coordinate N into planar three-coordinate N atoms.[31]

The extreme substitution inertness of the [Ru(L)($pyN_2H_2S_2$)] complexes and the very limited coordination chemistry of the [Fe($pyN_2H_2S_2$)] complex fragment on one hand, and the rich coordination chemistry of the [Fe(NHS_4)] complex fragment on the other hand, prompted us to return to complexes with [Fe(NS_4)] cores and to synthesize the pyS_4^{2-} ligand. As a first target complex, [Fe(CO)(pyS_4)] (**17**) was prepared. Complex **17** was obtained either by template alkylation of $[Fe(CO)_2(S_2C_6H_4)_2]^{2-}$ [32] with [py(CH_2OTs)$_2$] or from $FeCl_2 \cdot 4H_2O$ and pyS_4^{2-} in the presence of CO. Although the ν(CO) of **17** (1955 cm^{-1}) indicates a weaker Fe−CO bond in **17** than in [Fe(CO)($pyN_2H_2S_2$)] (**11**) (1928 cm^{-1}), **17** is stable toward Fe−CO dissociation in solid state as well as in solution.

General Spectroscopic Properties of Complexes. All complexes, with the exception of [Fe($pyN_2H_2S_2$)] (**10**) and [Ni(pyS_4)]$_2$ (**7**), are diamagnetic. They are soluble in DMF and DMSO, only moderately soluble in CH_2Cl_2 and usually insoluble in other common organic solvents. All complexes have been characterized by elemental analysis and IR, NMR, and mass spectra. The FD mass spectra exhibited either the molecular ions or ions resulting from loss of the coligands. The complexes with [M($pyN_2H_2S_2$)] cores exhibit either one unresolved broad or two weak ν(NH) IR bands in the region of 3290−3100 cm^{-1}. Characteristic IR bands are the very strong ν(CO) absorptions of **11** (1928 cm^{-1}), **14** (1927 cm^{-1}), and **17** (1955 cm^{-1}). The frequency of the strong ν(SO) IR bands of [Ru(DMSO)($pyN_2H_2S_2$)] (**12**) (1011 cm^{-1}) and [Ru(DMSO)($pyN_2H_2S_2$-Me_2)]I_2 (**15**) (1020 cm^{-1}) indicated S coordination of the DMSO ligands.[15] The $^{13}C\{^1H\}$ NMR spectra proved the most suitable spectroscopic probe for determining the symmetry of the complexes. Nine plus one ^{13}C NMR signals for the aromatic

(28) Sellmann, D.; Rohm, C.; Moll, M. *Z. Naturforsch.* **1995**, *50b*, 1729.
(29) Treichel, P. M.; Rosenhein, L. D. *Inorg. Chem.* **1981**, *20*, 942.
(30) Sellmann, D.; Becker, T.; Knoch, F. *Chem. Eur. J.* **1996**, *2*, 1072.
(31) Cameron, B. R.; House, D. A.; McAuley, A. *J. Chem. Soc., Dalton Trans.* **1993**, 1019.
(32) Sellmann, D.; Kreutzer, P.; Unger, E. *Z. Naturforsch.* **1978**, *33b*, 190.

Scheme 3. Syntheses of [M(L)($pyN_2H_2S_2$)] Complexes (M = Fe, Ru) and of [Fe(CO)(pyS_4)]

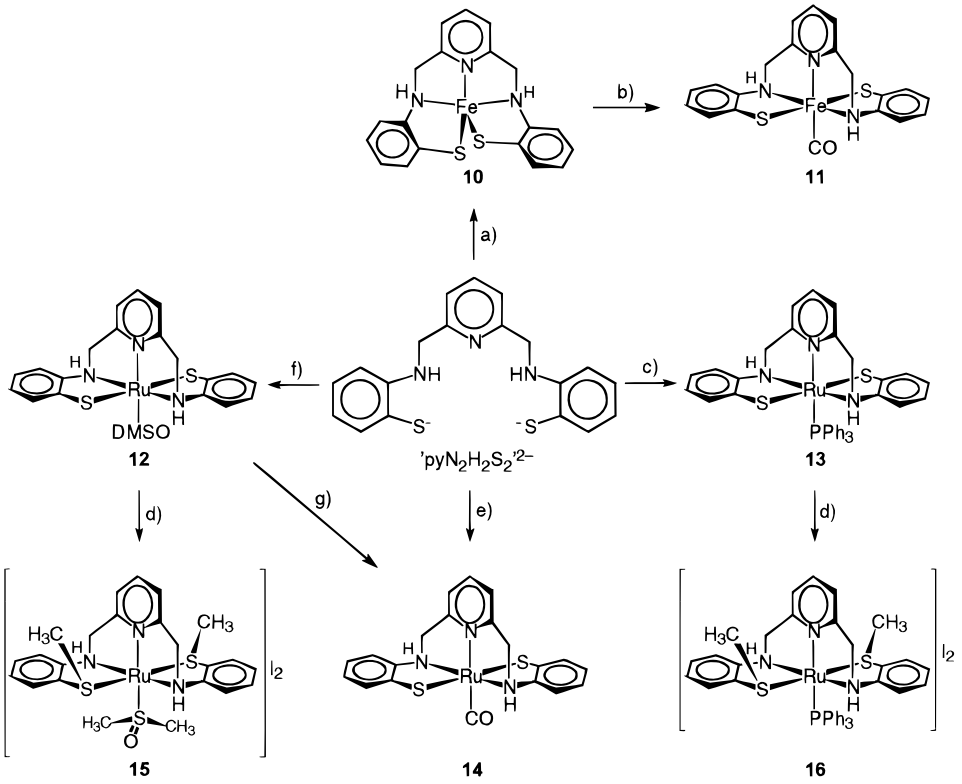

a) + $FeCl_2 \cdot 4\,H_2O$, MeOH / THF; b) + CO, 1 bar, 2 h, CH_2Cl_2; c) + $[RuCl_2(PPh_3)_3]$, THF, reflux, 2 h;
d) + exc. MeI, THF, 2 d; e) + $[Ru(H)(Cl)(CO)(PCy_3)_2]$, THF, reflux, 3 h; f) + $[RuCl_2(DMSO)_4]$, THF, reflux, 2 h;
g) + CO, 140 bar, THF, 120 °C, 12 h

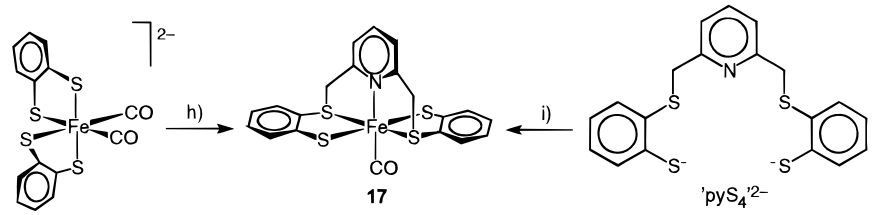

h) + $(C_5H_3N)(CH_2OTs)_2$, THF / MeOH, 24 h; i) + $FeCl_2 \cdot 4\,H_2O$, + CO, MeOH, 2 h

and the methylene C atoms of the chelate ligands clearly indicated C_2 symmetry for the [M(L)($pyN_2H_2S_2$)] complexes and [Fe(CO)(pyS_4)]. One ^{13}C NMR signal for the S methyl groups of **16** further indicated that *S*-alkylation of **13** had occurred in a diastereoselective way yielding only one diastereomer of **16**. The S−CH_3 ^{13}C NMR signal of **15** is distinctly broadened and probably consists of two unresolved singlets indicating the formation of two diastereomers, which were revealed by the X-ray structure determination of **15**. The ^1H NMR spectra, too, are consistent with C_2 symmetrical structures. For example, the chemically equivalent CH_2 protons of the free ligands become magnetically nonequivalent in [M($pyN_2H_2S_2$)] or [Fe(CO)(pyS_4)] (**17**) giving rise to two signals. In the case of **17**, these signals are split into doublets; in the case of [M(L)-($pyN_2H_2S_2$)] complexes the lower field doublet is further split into a doublet of doublets due to coupling with the adjacent NH proton.

X-ray Structure Determinations. X-ray structure analyses corroborated the spectroscopic results for several complexes. Figure 1 depicts the molecular structures of [Fe($pyN_2H_2S_2$)] (**10**) and [Fe(CO)(pyS_4)]·MeOH (**17**·MeOH). Table 2 lists selected distances and angles. The core structure of **10** is a distorted

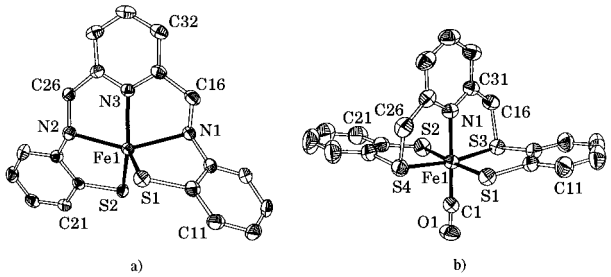

Figure 1. ORTEP diagrams of (a) [Fe($pyN_2H_2S_2$)] (**10**) and (b) [Fe-(CO)(pyS_4)]·MeOH (**17**·MeOH) (50% probability ellipsoids; H atoms and solvate molecules omitted).

trigonal bipyramid in which the pyridine donor N3 and the two thiolate donors occupy equatorial and the two amine donors N1 and N2 apical positions. Complex **10** exhibits approximate C_2 symmetry with the C_2 axis going through the Fe1−N3 bond. The [Fe(pyS_4)] core of pseudo-octahedral [Fe(CO)(pyS_4)] (**17**) also has approximate C_2 symmetry. The distinct difference of Fe−S and Fe−N distances in paramagnetic **10** vs diamagnetic **17** can plausibly be traced back to electrons in antibonding metal−ligand molecular orbitals.[5,9]

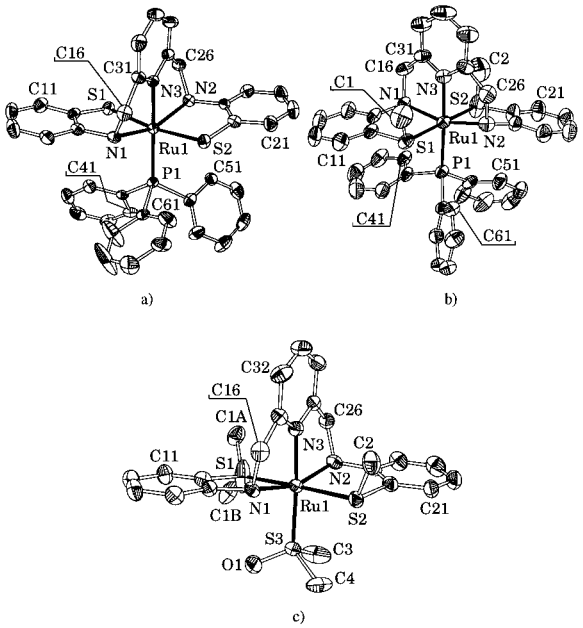

Figure 2. ORTEP diagrams of (a) $[Ru(PPh_3)(pyN_2H_2S_2)]\cdot 1.5THF$ (**13**·1.5THF), (b) the cation of $[Ru(PPh_3)(pyN_2H_2S_2\text{-}Me_2)]I_2\cdot CH_2Cl_2$ (**16**·CH_2Cl_2), and (c) the cation of $[Ru(DMSO)(pyN_2H_2S_2\text{-}Me_2)]I_{0.5}Cl_{1.5}\cdot 1.5CH_2Cl_2\cdot 0.5DMSO$ (**15′**·$1.5CH_2Cl_2$·0.5DMSO) (50% probability ellipsoids; H atoms and solvate molecules omitted).

Table 2. Selected Distances (pm) and Angles (deg) of $[Fe(pyN_2H_2S_2)]$ (**10**) and $[Fe(CO)(pyS_4)]\cdot MeOH$ (**17**·MeOH)

complex	**10**	**17**·MeOH	complex	**10**	**17**·MeOH
Fe1−N1	223.6(3)	201.4(2)	N3/S4−Fe1−S2	135.36(8)	90.26(5)
Fe1−S1	236.9(1)	231.1(2)	N2/S3−Fe1−S2	84.41(8)	87.43(5)
Fe1−S2	232.1(1)	228.9(2)	N2/S3−Fe1−S1	121.12(8)	89.87(5)
Fe1−N2/S3	226.4(3)	222.5(1)	N1−Fe1−N3/S4	75.41(11)	85.12(6)
Fe1−N3/S4	209.8(3)	223.2(1)	N1−Fe1−S2	107.01(8)	89.44(6)
Fe1−C1		175.7(2)	N1−Fe1−C1		178.19(8)

The Fe−S and Fe−N distances of **10** lie between those found in related high-spin and low-spin Fe(II) complexes.[5−9] For example, the Fe−S distances of **10** (236.9(1) and 232.1(1) pm) are longer than in **17** (*d*(Fe−S(thiolate)): 231.1(2) and 228.9(2) pm) but shorter than in high-spin $[Fe(N_2H_4)(NHS_4)]$ (*d*(Fe−S(thiolate)): 238.1(3) and 240.2(3) pm).

The closest analogue to **10** is high-spin $[Fe(NHS_4)]\cdot THF$,[8] which also has a pseudo-trigonal bipyramidal structure. The closest structural analogue to **17** is $[Fe(CO)(NHS_4)]$. Both **17** and $[Fe(CO)(NHS_4)]$ exhibit virtually identical Fe−S(thiolate) and Fe−S(thioether) distances. They differ in the Fe−N distances (**17**, 201.4(2) pm; $[Fe(CO)(NHS_4)]$, 207.2(8) pm) and in their symmetry. While **17** has approximate C_2 symmetry in solid state and C_2 symmetry in solution, $[Fe(CO)(NHS_4)]$ has, due to the $NH(C_2H_4)_2$ bridge, only C_1 symmetry in solid state and in solution.

Figure 2 depicts the molecular structures of the ruthenium complexes $[Ru(PPh_3)(pyN_2H_2S_2)]\cdot 1.5THF$ (**13**·1.5THF), $[Ru(PPh_3)(pyN_2H_2S_2\text{-}Me_2)]I_2\cdot CH_2Cl_2$ (**16**·CH_2Cl_2), and $[Ru(DMSO)(pyN_2H_2S_2\text{-}Me_2)]I_{0.5}Cl_{1.5}\cdot 1.5CH_2Cl_2\cdot 0.5DMSO$ (**15′**·$1.5CH_2Cl_2$·0.5DMSO). Selected distances and angles are listed in Table 3.

In all complexes the ruthenium centers are pseudo-octahedrally surrounded and the $[Ru(pyN_2H_2S_2)]$ cores exhibit approximate C_2 symmetry. Distances and angles show no anomalies. The Ru−S(thiolate) are only slightly longer than the Ru−S(thioether) distances (∼237 vs ∼233 pm), and the Ru−NH distances (∼213 pm) are distinctly longer than the Ru−N(pyridine) distances (∼201 pm). The relatively large difference in the Ru−N1 and Ru−N2 distances of **13** (211.9(4) vs 217.3(4) pm) is certainly due to crystal packing effects, because the NMR spectra unambiguously reveal C_2 symmetry for **13** in solution. The molecular structure of **15′** confirmed the S coordination of the DMSO ligand which had been indicated by the IR spectrum. Worth noting is the formation of only one diastereomer in the case of $[Ru(PPh_3)(pyN_2H_2S_2\text{-}Me_2)]^{2+}$ while two diastereomers in a ratio of 2:1 are formed in the case of the $[Ru(DMSO)(pyN_2H_2S_2\text{-}Me_2)]^{2+}$ cation. The 2:1 ratio of the two diastereomers follows from the disorder of the S1−CH_3 groups which could be refined with an A:B occupancy of 67(2):33(2)%. The formation of only one diastereomer in the case of the cation of **16** can be traced back to the sterically demanding PPh_3 ligand which allows nucleophilic attack of the thiolate donors only from one side.

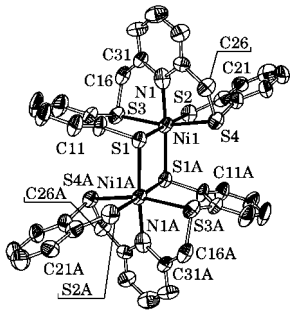

Figure 3. ORTEP diagram of $[Ni(pyS_4)]_2$ (**7**) (50% probability ellipsoids; H atoms omitted).

Table 3. Selected Distances (pm) and Angles (deg) of $[Ru(PPh_3)(pyN_2H_2S_2)]\cdot 1.5THF$ (**13**·1.5THF), $[Ru(PPh_3)(pyN_2H_2S_2\text{-}Me_2)]I_2\cdot CH_2Cl_2$ (**16**·CH_2Cl_2), and $[Ru(DMSO)(pyN_2H_2S_2\text{-}Me_2)]I_{0.5}Cl_{1.5}\cdot 1.5CH_2Cl_2\cdot 0.5DMSO$ (**15′**·$1.5CH_2Cl_2$·0.5DMSO)

complex	**13**·1.5THF	**16**·CH_2Cl_2	**15′**·$1.5CH_2Cl_2$·0.5DMSO
Ru1−N1	211.9(4)	214.1(4)	213.4(6)
Ru1−N2	217.3(4)	214.4(4)	213.5(6)
Ru1−N3	201.2(4)	203.8(4)	199.5(5)
Ru1−S1	236.5(2)	234.8(2)	232.4(2)
Ru1−S2	238.0(2)	232.5(2)	234.0(2)
Ru1−P1/S3	230.1(1)	237.4(1)	227.0(2)
N1−Ru1−S1	85.0(1)	83.6(1)	83.8(2)
N2−Ru1−S1	92.1(1)	98.4(1)	95.2(2)
N2−Ru1−S2	83.3(1)	83.9(1)	84.0(2)
N3−Ru1−N1	78.9(2)	79.4(2)	79.7(2)
N3−Ru1−S1	86.8(1)	93.2(1)	91.7(2)
N3−Ru1−P1/S3	170.7(1)	177.7(1)	176.3(2)

Table 4. Selected Distances (pm) and Angles (deg) of $[Ni(pyS_4)]_2$ (**7**)

Ni1−N1	206.0(8)	S4−Ni1−S2	87.5(1)
Ni1−S1	239.6(3)	S3−Ni1−S2	92.9(1)
Ni1−S2	238.1(3)	S3−Ni1−S1	87.07(9)
Ni1−S3	239.7(3)	N1−Ni1−S4	82.5(2)
Ni1−S4	237.5(3)	N1−Ni1−S2	93.3(2)
Ni1−S1A[a]	244.8(3)	N1−Ni1−S1A	173.4(2)

[a] Symmetry code: $-x, -y + 2, -z + 1$.

Figure 3 depicts the molecular structure of $[Ni(pyS_4)]_2$ (**7**) which had been obtained as intermediate in the pyS_4-H_2 synthesis. Table 4 lists selected distances and angles.

The dinuclear $[Ni(pyS_4)]_2$ (**7**) exhibits crystallographically imposed inversion symmetry. The nickel centers are pseudo-octahedrally coordinated, the $[Ni(pyS_4)]$ cores are approximately C_2 symmetrical, and bridged via thiolate donors. The Ni−S thiolate and thioether distances in the range of 237−240 pm are typical for paramagnetic six coordinate nickel complexes

Scheme 4. Donor Atom Sets, Core Structures and ν(CO) Frequencies (cm^{-1}) of [Fe(CO)L] Complexes (L = S_5^{2-}, NHS_4^{2-}, pyS_4^{2-}, $N_2H_2S_3^{2-}$, $N_3H_3S_2^{2-}$, $pyN_2H_2S_2^{2-}$)

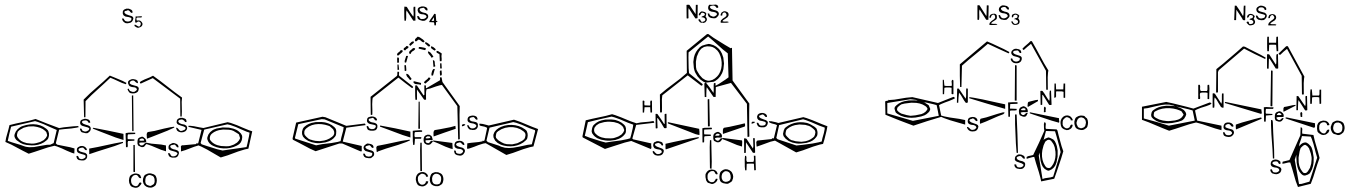

and have also been found in the closely related $[Ni(NHS_4)]_2$.[33] The Ni−N(pyridine) distances in **7** (206.0(8) pm) are (expectedly) shorter than Ni−N distances to aliphatic NH donors such as in $[Ni(NHS_4)]_2$ (d(Ni−N): 214.4(7) pm).

The structures of all complexes described here demonstrate that the C_2 symmetrical core structures can be considered a typical feature of $[M(pyN_2H_2S_2)]$ and $[M(pyS_4)]$ fragments because they are maintained over a wide range of metal donor distances in both five- and six-coordinate complexes which can be diamagnetic or paramagnetic.

Influence of Donor Atom Sets and Core Structures upon the Metal Electron Density in Six-Coordinate [Fe(CO)(N_xS_y)] Complexes ($x + y = 5$). The ligands and iron carbonyl complexes described in this and preceding papers[34,35] render it possible to estimate the influence of donor atom sets and core structures upon the electron density at the iron centers. The ν(CO) frequency of the complexes is used as a probe and [Fe(CO)(S_5)] (S_5^{2-} = 2,2′-bis(2-mercaptophenylthio)diethyl sulfide(2−)) as the starting complex. Scheme 4 schematically depicts the structures of the relevant complexes and demonstrates that exchange of aliphatic thioether S atoms for either aliphatic N or pyridine N donors does not significantly change the ν(CO) frequencies in [Fe(CO)(S_5)] (1960 cm^{-1}) and [Fe(CO)(NHS_4)] (1960 cm^{-1}) or [Fe(CO)(pyS_4)] (1955 cm^{-1}). (The Fe−S distances within the $[FeS_4]$ planes of these three complexes also remain approximately identical.)

The ν(CO) decrease of 27 cm^{-1} between [Fe(CO)(pyS_4)] and the isostructural [Fe(CO)($pyN_2H_2S_2$)] allows a conclusion that the comparable ν(CO) difference of 26−28 cm^{-1} between [Fe(CO)(NHS_4)] (1960 cm^{-1}) and [Fe(CO)($N_2H_2S_3$)] (1932 cm^{-1}) or [Fe(CO)($N_3H_3S_2$)] (1934 cm^{-1}) is rather due to the exchange of aromatic thioether S by aromatic NH donors than caused by different core structures.

Conclusion

The primary aim of this work was the synthesis of the new ligands $pyN_2H_2S_2^{2-}$ and pyS_4^{2-} in order to introduce steric constraints into iron and ruthenium complexes with either $[MN_3S_2]$ or $[MNS_4]$ cores. Variation of the electron density at the metal centers and enforced trans coordination of the thiolate donors as found in low-spin [Fe(L)(NHS_4)] complexes (L = CO, PR_3, N_2H_2) were intended to favor the coordination of nitrogenase related small molecules including N_2.

The results show that increasing the number of N donors increases the electron density at the metal centers of complexes with $[M(L)(N_xS_y)]$ cores. Exchange of aromatic thioether S vs aromatic amine NH donors has a major effect in comparison to an exchange of aliphatic thioether S vs NH and pyridine N donors or to a change of the metal donor core structure. The introduction of $[py(CH_2)_2]$ bridges into the pentadentate N_xS_y ligands caused steric constraints insofar as all complexes with $[M(pyN_2H_2S_2)]$ or $[M(pyS_4)]$ fragments invariably exhibit C_2 symmetrical core structures and trans coordination of the thiolate donors as found in the low-spin [Fe(L)(NHS_4)] complexes (L = CO, PR_3, NO^+, N_2H_2, etc.).

The steric constraints and the increase of the metal electron density effected by a growing number of N donors do not necessarily lead to kinetically more stable M−L bonds in $[M(L)(N_xS_y)]$ complexes. This result, which we cannot plausibly explain yet, is demonstrated by the pair of [Fe(CO)($pyN_2H_2S_2$)] and [Fe(CO)(pyS_4)] complexes. Although the ν(CO) bands indicate stronger Fe−CO bonds in [Fe(CO)($pyN_2H_2S_2$)] than in [Fe(CO)(pyS_4)], [Fe(CO)($pyN_2H_2S_2$)] is much more labile than [Fe(CO)(pyS_4)] toward CO dissociation. The ability of the $[Fe(pyN_2H_2S_2)]$ fragment to coordinate ligands other than CO is as limited as that of the related $[Fe(N_2H_2S_3)]$ or $[Fe(N_3H_3S_2)]$ fragments, which have a different core structure.

The complex fragment $[Ru(pyN_2H_2S_2)]$ is slightly more versatile in binding various coligands, but the resulting complexes proved extremely substitution inert and did not yield nitrogenase related series of complexes with N_xH_y ligands either. More detailed investigations of the $[Fe(pyS_4)]$ fragment, which is analogous to the $[Fe(NHS_4)]$ fragment, but sterically preorganized, are being carried out in order to test its binding capability toward nitrogenase related small molecules.

Acknowledgment. Support of these investigations by the Deutsche Forschungsgemeinschaft and Fonds der Chemischen Industrie is gratefully acknowledged.

Supporting Information Available: X-ray crystallographic data, in CIF format, for compounds **7**, **10**, **13**·1.5THF, **15′**·1.5CH_2Cl_2·0.5DMSO, **16**·CH_2Cl_2, and **17**·MeOH. This material is available free of charge via the Internet at http://pubs.acs.org. Crystallographic data (excluding structure factors) for the structures reported in this paper have been deposited with the Cambridge Crystallographic Data Centre as depository nos. 132879 (**7**), 132880 (**10**), 132881 (**13**·1.5THF), 132882 (**15′**·1.5CH_2Cl_2·0.5DMSO), 132883 (**16**·CH_2Cl_2), and 132884 (**17**·MeOH). Copies of the data can be obtained free of charge upon application to The Director, CCDC, 12 Union Road, Cambridge, CB2 1EZ, UK (fax: int. code +44(1223)336-033, E-mail: deposit@chemcrys.cam.ac.uk).

IC990169H

(33) Sellmann, D.; Fünfgelder, S.; Knoch, F. *Z. Naturforsch.* **1991**, *46b*, 1593.
(34) Sellmann, D.; Binker, G.; Moll, M.; Herdtweck, E. *J. Organomet. Chem.* **1987**, *327*, 403.
(35) Sellmann, D.; Kleine-Kleffmann, U. *J. Organomet. Chem.* **1983**, *258*, 315.